HHS Public Access

Author manuscript

Obesity (Silver Spring). Author manuscript; available in PMC 2016 November 01.

Published in final edited form as:

Obesity (Silver Spring). 2015 November ; 23(11): 2142–2148. doi:10.1002/oby.21248.

Radiologic evidence that hypothalamic gliosis is associated with obesity and insulin resistance in humans

Ellen A. Schur[1], **Susan J. Melhorn**[1], **Seok-Kyun Oh**[2], **J. Matthew Lacy**[3], **Kathryn E. Berkseth**[4], **Stephan J. Guyenet**[4], **Joshua A. Sonnen**[3], **Vidhi Tyagi**[1], **Mary Rosalynn B. De Leon**[1], **Mary F. Webb**[5], **Zenobia T. Gonsalves**[1], **Corinne L. Fligner**[3], **Michael W. Schwartz**[4], and **Kenneth R. Maravilla**[2]

[1]Department of Medicine, Division of General Internal Medicine, University of Washington; Seattle, WA

[2]Department of Radiology, University of Washington; Seattle, WA

[3]Department of Pathology, University of Washington; Seattle, WA

[4]Department of Medicine, Division of Metabolism, Endocrinology and Nutrition, University of Washington; Seattle, WA

[5]Department of Epidemiology, University of Washington; Seattle, WA

Abstract

Objective—To utilize quantitative magnetic resonance imaging (MRI) to test whether mediobasal hypothalamic (MBH) gliosis is associated with obesity and insulin resistance in humans.

Methods—Sixty-seven participants underwent a fasting blood draw and MRI. Cases with radiologic evidence of MBH gliosis (N=22) were identified as the upper tertile of left MBH T2 relaxation time and were compared to controls (N=23) from the lowest tertile. In a separate postmortem study, brain slices (N=10) through the MBH were imaged by MRI and stained for glial fibrillary acidic protein (GFAP).

Results—In all participants, longer T2 relaxation time in the left MBH was associated with higher BMI (P=0.01). Compared to controls, cases had longer T2 relaxation times in the right MBH (P<0.05), as well as higher BMI (P<0.05), fasting insulin concentrations (P<0.01), and HOMA-IR values (P<0.01), adjusted for sex and age. Elevations in insulin and HOMA-IR were also independent of BMI. In the postmortem study, GFAP staining intensity was positively

Contact Info: Ellen Schur, MD, MS, Harborview Medical Center, 325 Ninth Ave, Box 359780, Seattle, WA 98104 Phone: 206-744-1830 Fax: 206-744-9917 ellschur@u.washington.edu.

Disclosure. The authors have nothing to disclose.

Author Contributions. EAS developed hypotheses, designed experiments, obtained grants, analyzed data, and wrote the manuscript. SJM developed image analysis techniques, analyzed data, and wrote the manuscript. S-KO designed and executed the MR imaging in autopsy samples. JML designed autopsy specimen processing techniques and, along with JAS, executed hypothalamic sectioning and evaluated histology sections. KEB reviewed medical records, and, along with SJG, coordinated histological analyses. VT, MBDL, MFW and ZTG conducted human studies. CF contributed to experimental design of autopsy study. MWS contributed to experimental design and data interpretation, obtained grants, and reviewed and edited the manuscript. KRM contributed to the design of the experiments, directed the imaging of the autopsy samples, designed all MR acquisitions, and reviewed and edited the manuscript.

associated with MBH T2 relaxation time ($P<0.05$), validating an MRI-based method for the detection of MBH gliosis in humans.

Conclusions—These findings link hypothalamic gliosis to insulin resistance in humans and suggest that the link is independent of the level of adiposity.

Keywords

gliosis; magnetic resonance imaging (MRI); hypothalamus; obesity; insulin resistance

Introduction

A growing literature in rodent models suggests that obesity is associated with inflammation of and injury to hypothalamic areas critical to the control of energy balance and glucose metabolism (1-5). Histologically, this response is characterized by gliosis, the proliferation and activation of glial cells induced in response to central nervous system (CNS) injury. Microscopically, gliosis involves infiltration of microglia, activation of microglia and astrocytes, and astrocytic proliferation, including increased density of astrocyte processes on cell bodies of neurons. Feeding rodents a high-fat diet triggers inflammation and gliosis in the arcuate nucleus, located in the mediobasal hypothalamus (MBH), even before obesity occurs (1,4) and eventually, reduces pro-opiomelanocortin cell numbers (1). Such changes are associated with both obesity and impaired glucose homeostasis in rodents (5-7), and they offer an explanation for obesity-associated resistance of hypothalamic neurons to humoral signals, such as leptin and insulin (8,9). Despite the mounting evidence from animal studies, the translational significance of hypothalamic gliosis for obesity is largely unknown (10) and no human studies have examined the relationship between hypothalamic gliosis and measures of glucose homeostasis.

A core concept of the current research is that gliosis can be detected in humans using magnetic resonance imaging (MRI) by assessing for increased signal intensity (brightness) on a T2-weighted image (11-13). Clinically, the visual identification of increased T2 signal intensity is used to detect CNS insults, like stroke and multiple sclerosis (13,14), but quantitative techniques can detect more subtle alterations in CNS tissue characteristics (2,11). One prior retrospective study in humans utilized clinical MRI examinations and found a positive association between body mass index (BMI) and a ratio of T2 signal in the MBH as compared to the amygdala (1). In the current studies, we applied a quantitative MRI technique to measure T2 relaxation time in the MBH, employing a dedicated sequence not typically utilized in clinical imaging protocols. Using a similar sequence, we found longer MBH T2 relaxation times in diet-induced obese (DIO) mice compared to chow-fed controls (2,15). Here, in two separate studies, we sought evidence for MBH gliosis in humans. Study 1, an *in vivo* MRI study, hypothesized that MBH gliosis, when present, would be associated with obesity and insulin resistance. Study 2, a postmortem study of human brain tissue, hypothesized that T2 relaxation time would be related to immunohistochemical measures of astrocytosis in the MBH.

Methods

Study 1, a nested case-control design, identified cases with MBH gliosis (the “disease” under investigation) and compared them to “non-diseased” (no evidence of gliosis) participants derived from the same population. Case-control designs are useful to ascertain risk factors for or attributes of a disease, and our intent was the latter. We defined cases as the tertile of participants with the longest T2 relaxation times in the left MBH and compared their characteristics to control participants within the tertile with the shortest T2 relaxation times in the same brain area. The left MBH was selected based on our previous asymmetrical results, which indicated a stronger relationship between elevated T2 signal and BMI on the left than right (1). Study 2 is a cross-sectional examination in postmortem human hypothalamus of the histopathological correlation between MBH T2 relaxation time and immunohistochemical markers of gliosis.

Participants

Study 1—Male and female participants aged 18-50 years were recruited. Exclusion criteria included: history of obesity (as determined by self-report of lifetime maximum weight) if currently non-obese (BMI 18-29.9 kg/m^2); history of bariatric surgery; current dieting for weight loss; chronic disease including diabetes; use of metabolism-altering medications; pregnancy or breastfeeding; heavy alcohol use; smoking; and MRI contraindications including weight >330 lbs. Seventy individuals underwent the MRI protocol, and three were excluded due to pulsatile flow artifacts in the MBH.

Study 2—Adult autopsy cases performed at the UW Medical Center between June 2010 and December 2012 were evaluated for inclusion criteria: the autopsy consent allowed research use; an intact hypothalamus sectioned in a manner conducive to imaging; and aged between 18-70 years. Clinical charts were reviewed for exclusion criteria: an abnormal postmortem brain examination; clinical history of a neurodegenerative or neuro-inflammatory disease, anoxic injury, or other CNS disease; severe cachexia; or a history of weight-loss surgery.

All studies and procedures were approved by the UW Human Subjects Division. Participants provided written informed consent.

Procedures

Study 1—Participants arrived after a 10-hour fast; had a morning blood draw, and height and weight measurements; answered behavioral questionnaires; and underwent an MRI.

Behavioral questionnaires: The International Physical Activity Questionnaire (IPAQ) Short Form assessed physical activity (www.ipaq.ki.se). The Revised Restraint Scale (16) and Three-Factor Eating Questionnaire (17) assessed eating behaviors.

Glucose and hormone analysis: Glucose levels were measured with an oxidase/O2 electrode method or a hexokinase method. Insulin levels were determined by immunoenzymatic methods. The homeostatic model assessment for insulin resistance (HOMA-IR) was calculated (18).

Image acquisition: All scans were acquired on a 3-Tesla Philips Achieva MR scanner (version 3.2, Philips Medical Systems, Best, The Netherlands) using a 32-channel head radiofrequency coil. Sequences included a T1-weighted scan and a quantitative multi-slice/multi-echo T2-weighted sequence with 16-echoes (interecho spacing of 10 ms) (TR/TE/NSA: 2000/20-170/1). Slices were acquired from the optic chiasm through the mammillary bodies (9-12 slices/subject, slice thickness=2.5 mm, inter-slice gap=0.0-0.2 mm). In-plane pixel resolution was 0.70-0.80×0.75-0.86 mm resulting in an acquired voxel size of 1.313-1.720 mm^3. T2 relaxation time was calculated from the signal decay curve of the 16 echoes on a pixel-by-pixel basis and displayed as a quantitative T2 relaxation time parametric map to evaluate regional tissue T2 values.

MRI analysis: The coronal slice immediately posterior to the optic chiasm encompassing the rostral arcuate nucleus, was identified for each subject (19). Within the same slice, reference regions of interest (ROIs) in the putamen and amygdala were identified. ROIs were placed on high resolution coronal images (Figure 1A-B) and then were transferred to the T2 parametric map (Figure 1C). Mean±SD T2 relaxation time per ROI was recorded (OsiriX Imaging Software, version 5.6).

Study 2—The coronal brain slice that included the entire hypothalamus was placed in a shallow plastic container, submerged in water, and placed in a multichannel human knee coil for imaging in the 3T system.

Image acquisition and analysis: The imaging sequences described above were modified as follows: a quantitative 16-echo T2 spin-echo sequence was performed in a coronal plane parallel with the brain slice (TR/TE/NSA: 2000/20-170/4). In-plane resolution of 0.8×0.8 mm that was zero-filled to yield an interpolated resolution of 0.25×0.25 mm per pixel and 2 mm slice thickness (0 gap) resulting in a voxel size of 0.156 mm^3. Image analysis was identical to Study 1.

Tissue preparation and immunohistochemistry: A 2×2 cm of formalin-fixed brain tissue from the brain slice used for MR imaging was blocked (from the optic chiasm to the mammillary bodies) (19), bisected in its coronal midline, and serially sectioned (4 μm thickness) either posterior to anterior, or anterior to posterior. Every third section was stained with hematoxylin and eosin (H&E) and examined for localization of the arcuate nucleus and other abnormalities, such as inflammation, neoplasia, and malformations.

Adjacent slides from H&E-identified sections through the arcuate nucleus were processed for glial fibrillary acidic protein (GFAP) immunoreactivity (Leica BOND-III, Leica Microsystems, Inc., Buffalo Grove, IL). Slides were incubated with monoclonal mouse anti-human GFAP (dilution 1:150, DAKO, Glostrup, Denmark), and visualized with a horseradish peroxidase complex using 3.3'-diaminobenzidine (DAB). Hematoxylin was applied as a nuclear counterstain.

Image capture and analysis: H&E and GFAP-stained slides of the MBH were digitally scanned with an Aperio ScanScope CS (Leica Biosystems Aperio ePathology, Vista, CA). ROIs, targeting the MBH and approximating the placement to the MRI T2 parametric map,

were drawn on each image. Negative annotations were drawn to exclude large vessels, tissue artifacts, and areas of edge effect background staining from the analysis.

Immunohistochemical staining of GFAP within the ROIs was evaluated using a color deconvolution area quantification algorithm (Aperio Brightfield Image Analysis Toolbox software). Briefly, RGB color vectors for the nuclear (hematoxylin) and positive (DAB) stains were measured from the slides for input as parameters. The algorithm was calibrated with the RGB color vectors, and the DAB stain was selected as the positive stain to be quantified. The lower weak positive staining threshold was calibrated to include all tissue stained with hematoxylin or DAB. The medium positive threshold was configured by observing regions on multiple stained slides, and the value was adjusted to only include positive GFAP stained filament/process areas. The Color Deconvolution analysis software measured surface area and density of positive staining. The combined Medium+Strong percent surface area, Average Optical Density (OD) of Medium+Strong regions (stain intensity), and Average OD*Percent Positive of Medium+Strong regions were calculated. OD is computed as $-LOG(I_0/I)$, whereas I is the input intensity of light (240 for Aperio ScanScope scanners) and I_0 is the measured intensity of light received at the camera. OD is a measurement of absorbance and is directly related to the concentration of stain in the tissue sample.

Statistical analysis

Data are reported as mean±SEM, unless otherwise noted. Chi-squared tests of proportions were used for categorical variables. Linear mixed models capable of accounting for repeated measures were used to evaluate regional and laterality differences in mean T2 relaxation time. Group differences were tested by using multiple linear regression to adjust for covariates. Least square means were calculated for adjusted models. Simple linear regression models were applied to evaluate associations and Pearson's correlation coefficients were calculated for descriptive purposes. Bilateral MBH data were averaged for Study 2 histologic and MRI parameters. Analyses were performed with STATA v.13.1 (College Station, TX).

Results

Study 1

Participant characteristics—The sample included 67 individuals (31 men, 36 women) aged 19-50 years. BMI ranged from 19-45 kg/m^2 (mean 30±0.9 kg/m^2). From within this cohort, 22 cases with evidence of MBH gliosis were identified and compared to controls without evidence of MBH gliosis (N=23). There were no significant differences in the proportion of women (chi^2(1)=1.79, P=0.18) or participants with obesity (chi^2(1)=2.70, P=0.10) between cases and controls, nor were there differences in age (P=0.46), eating behavior (P=0.24-0.50), total physical activity (P=0.52), or time spent sitting (P=0.65) (Table 1).

Measurement of T2 relaxation time in the MBH of humans—Among all 67 participants, mean±SEM bilateral T2 relaxation time for the MBH was 94.3±0.8 ms. T2

relaxation times were longer in the MBH than in the amygdala (81.8±0.4 ms) or putamen (60.0±0.4 ms; P<0.0001). There was no main effect of laterality (P=0.66) and no asymmetry in the MBH specifically (right: 94.3±1.1 ms; left 94.5±0.8 ms). There were no sex differences in mean T2 relaxation time in any ROI (data not shown). Normal, age-related declines in T2 relaxation time (20) were observed in reference regions (amygdala: left β= −0.11 ms, P=0.013, right β=−0.14 ms, P=0.002; putamen: left β=−0.25 ms, P<0.001, right β=−0.26 ms, P<0.001) but not in the MBH (left β=0.11 ms, P=0.17; right β=−0.09 ms, P=0.41).

In the left MBH, longer T2 relaxation time was associated with higher BMI and HOMA-IR scores (BMI: β=0.28 ms 95%CI: 0.07- 0.50, P=0.01; HOMA-IR: : β= 1.48 ms 95%CI: 0.48- 2.5, P<0.01; Figure 2), but not on the right (BMI: β= −0.07 ms 95%CI: −0.35- 0.22, P=0.65; HOMA-IR: β= 0.40 ms 95%CI: −0.93- 1.7, P=0.55). Neither BMI nor HOMA-IR were associated with T2 relaxation time in any of the reference regions, except for BMI and the right amygdala (β= −0.18 ms 95%CI: −0.30- −0.05, P<0.01). Multiple regression analysis confirmed the relationship of both BMI and HOMA-IR to T2 relaxation time in the left MBH to be independent of age, sex, and physical activity (data not shown).

Case-control study of attributes of MBH gliosis—All models were adjusted for sex and age. Cases, by definition, had higher T2 relaxation times in the left MBH compared to controls (102±0.9 vs. 88.5±0.9 ms, P<0.0001). Cases also had longer T2 relaxation times in the right MBH (98.5±2.0 vs. 92.7±2.0 ms, P<0.05, Figure S1), suggesting that when evidence for gliosis is strong it is a bilateral phenomenon. Mean BMI was higher compared to controls (Figure 3A). There were no group differences in the mean T2 relaxation time in reference regions (amygdala and putamen) between cases and controls (Figure S1).

There was no difference in mean fasting plasma glucose concentration between groups (Figure 3B). Fasting plasma insulin concentrations and HOMA-IR were significantly higher among cases than controls (Figure 3C-D). In order to examine if these differences were independent of BMI, a fully adjusted model included BMI as a covariate (with sex and age). Fasting insulin levels remained significantly higher among cases compared to controls (10.5±0.97 vs. 7.15±0.95 μIU/mL, P=0.02) as did HOMA-IR (2.53±0.24 vs. 1.69±0.24, P=0.02), signifying that the increased insulin resistance among cases was independent of obesity *per se*.

Study 2

Neuropathological correlation of T2 relaxation time with immunohistochemical analyses—Fifteen postmortem brain slices were imaged for measurement of T2 relaxation time (Figure 4B). Similar to the *in vivo* findings described above, T2 relaxation time was longer in the MBH than in either the amygdala or putamen (P<0.0001). There was no effect of laterality (P=0.72).

A subset of samples (N=10) were successfully sectioned through the arcuate nucleus of the hypothalamus. These sections were histologically processed for GFAP immunostaining (Figure 4A, C-F) and evaluated for GFAP staining intensity (mean optical density: 0.33±0.03), area of staining (mean % GFAP positive: 62±14), and a combined measure of

area*intensity (mean: 21±7). GFAP staining intensity was positively associated with mean T2 relaxation time in the bilateral MBH (r=0.71, P=0.02). Trends were also present between MBH T2 relaxation time and the total stained area (r=0.62, P=0.06) and between a combined measure of staining intensity and area (r=0.58, P=0.08). Given potential sex and age-related changes in arcuate nucleus tissue characteristics (19), an exploratory analysis was performed that included these factors as covariates in the models. Results demonstrated a strengthening of associations between MBH T2 relaxation time and measures of GFAP staining intensity (P=0.01), staining area (P=0.03), and combined area and intensity (P=0.02).

Discussion

Clinical MRI exams generally rely on visual inspection to determine the presence or absence of gliosis, based on areas of brightness (high T2 signal) on T2-weighted images. The quantitative approach applied in this study is distinct from routine clinical examinations as it was designed to detect more subtle changes in the hypothalamic T2 signal than is possible by qualitative visual evaluation. Our findings extend previous evidence that the MBH T2 signal is positively correlated with BMI (1). Moreover, we determined that cases who had the highest MBH T2 signal intensity showed signs of insulin resistance, even after adjusting for differences in BMI. To our knowledge, this is the first evidence of a relationship between MBH gliosis in humans and the presence of insulin resistance, independent of the degree of adiposity. This observation is consistent with the broader view that hypothalamic dysfunction is a feature of the obese, insulin-resistant phenotype in humans.

This study identified both radiologic and histologic evidence for MBH gliosis in humans. Our MRI outcomes indicate that in the MBH, tissue structure is altered differentially from reference regions. T2 relaxation times were longer in the MBH in both the *in vivo* and postmortem studies, which is consistent with but does not definitively identify gliosis. In prior studies, longer T2 relaxation times were related to increased glial cell numbers (11,21), reactive astrocytosis (22), and decreased neuronal populations (11). Importantly, one prior study showed histologically that longer T2 relaxation time was associated with increased astrocyte density among high-fat diet fed animals (2). Our findings expand upon this work by providing evidence, in humans, for astrocyte proliferation and activation in the MBH and for a histopathologic correlation between MBH T2 relaxation time and the extent of astrocytosis. Thus, previous studies and the current findings attest to both the presence of MBH gliosis in humans and the ability of quantitative MRI techniques to detect MBH gliosis.

The positive correlation found between BMI and T2 relaxation time is consistent with a possible role for hypothalamic inflammation and gliosis in the development and persistence of human obesity (1,23). However, not all individuals with obesity in our study demonstrated gliosis, and evidence for gliosis was identified in some participants whose BMI was within the normal range. Although the interpretation of these findings awaits further study, we postulate that obesity is a relatively crude marker for the presence of hypothalamic gliosis, but when MBH gliosis is present, metabolic health deteriorates. In fact, studies in rodents show consuming a high-fat diet causes hypothalamic inflammation

and gliosis that precedes the development of obesity (1-5). Conversely, increasing physical activity or switching from a high-fat diet to a standard chow diet can alleviate both obesity and gliosis in mice (24,25) indicating that hypothalamic gliosis is potentially reversible, at least in mice. Longitudinal studies to address the reversibility of hypothalamic gliosis in humans are therefore a high priority. Similarly, the underlying cause of MBH gliosis in humans is unknown, and the question of whether MBH gliosis in normal-weight individuals increases the future risk of obesity or type 2 diabetes mellitus remains unanswered.

Cases with the strongest radiologic evidence for MBH gliosis also had elevations of both fasting plasma insulin levels and HOMA-IR that were not fully explained by their higher BMIs. These data in humans echo evidence from animal models showing that glucose homeostasis might be impaired independently by inflammatory responses in the hypothalamus (5,26). The MBH and specifically, the arcuate nucleus, play a critical role in the regulation of energy homeostasis, glucose metabolism (27), and non-insulin-mediated glucose disposal (28,29). Neurons within the arcuate nucleus sense and respond to a variety of humoral inputs relevant to nutrient status, including leptin, insulin and glucose (30,31), and disruption of these signaling pathways promotes metabolic dysregulation (32). Hypothalamic inflammation in rodent models of DIO is associated with reduced neuronal signaling by both insulin and leptin, which may in turn contribute to the development and maintenance of obesity, insulin resistance, and glucose intolerance (33-35). However, whether specific neurocircuits involved in energy and glucose metabolism are disturbed in humans with MBH gliosis remains unanswered, a possibility that has been the focus of recent reviews (28,36). These findings support theories that obesity-associated metabolic impairment, perhaps ultimately leading to type 2 diabetes, is linked to structural changes in the hypothalamus.

There are important limitations to these studies. First, increased T2 signal is the signature appearance of gliosis on MRI (11,21,22), however factors other than gliosis can affect T2 relaxation time, including infection, tumor, ischemic damage, and auto-immune inflammatory disease. Such mechanisms are unlikely to explain our findings, however, given that only healthy participants were enrolled and our findings from the human autopsy samples link immunohistochemical evidence for astocytosis to radiologic findings. Second, the arcuate nucleus has indistinct radiologic demarcations, and portions of other hypothalamic nuclei could have been included in our MBH ROIs. Third, this and prior studies have shown stronger results in the left MBH (1). Although lateralization requires further study, it would be consistent with evidence that hypothalamic white matter connections are lateralized in humans (37), as is cerebral autonomic function, with parasympathetic output predominating in the left hemisphere (38). It is therefore conceivable that projections of MBH neurons to parasympathetic nervous system outflow pathways (which may contribute to glucoregulation) are similarly lateralized, and could impact MBH susceptibility to inflammation and injury. Additional studies are needed to either confirm or reject lateralization of gliosis detected by MRI and if confirmed, to identify underlying mechanisms. Fourth, Study 2 focused on validating MRI-based detection of astrocytosis in humans, but future work would benefit from evaluating obesity history in relation to histologic findings and broadening tissue analyses to examine microglia and neuronal populations. In the current sample, weight changes related to underlying illnesses

and fluid shifts during hospitalization precluded an accurate assessment of body weight in all subjects. Finally, the data are cross-sectional and can speak neither to the risk factors nor to the long-term implications of MBH gliosis.

Based on the current work, MRI is useful for investigating the role of MBH gliosis in the pathogenesis and maintenance of human obesity and its associated metabolic impairments. Future work should employ more quantitative tools to investigate changes in glucose metabolism and insulin action associated with MBH gliosis in humans. Recent animal data suggest that when obesity is reversed by switching from a high-fat to a low-fat diet, MBH gliosis also reverses (25). Since human obesity is notoriously difficult to reverse non-surgically (39,40), it is of strong interest for future studies to determine whether obesity-associated MBH gliosis is reversible in humans and if MBH gliosis contributes to the physiologic defense of higher body weights in obesity or weight regain after weight loss. New avenues for treatment or prevention of obesity may be revealed by addressing these fundamental questions.

Supplementary Material

Refer to Web version on PubMed Central for supplementary material.

Acknowledgments

The authors thank Jonathan Henrikson of the UW Pathology Digital Imaging Core Facility for technical assistance. This study used Digital Imaging Services through Northwest BioTrust--supported by the National Cancer Institute (P30CA015704, PI: F.Appelbaum), Life Sciences Discovery Fund (Washington Phenotyped Biospecimen Resource, PI: J.Slattery and Consortium Biospecimen Program, PI: P.Porter), Fred Hutchinson Cancer Research Center, UW School of Medicine, and Department of Pathology.

Funding. This work was supported by the National Institutes of Health award numbers R01DK089036 (EAS), R01DK052989 (MWS), T32DK007247 (KEB) and K12HD053984 (KEB), the American Diabetes Association award number 1-13-IN-47 (EAS), the Nutrition Obesity Research Center at the University of Washington award number P30DK035816 and a University of Washington Royalty Research Fund Award (EAS).

REFERENCES

1. Thaler JP, Yi CX, Schur EA, Guyenet SJ, Hwang BH, Dietrich MO, et al. Obesity is associated with hypothalamic injury in rodents and humans. Journal of Clinical Investigation. 2012; 122(1):153–62. [PubMed: 22201683]
2. Lee D, Thaler JP, Berkseth KE, Melhorn SJ, Schwartz MW, Schur EA. Longer T2 relaxation time is a marker of hypothalamic gliosis in mice with diet-induced obesity. American Journal of Physiology. Endocrinology and Metabolism. 2013; 304(11):E1245–50. [PubMed: 23548614]
3. Guyenet SJ, Nguyen HT, Hwang BH, Schwartz MW, Baskin DG, Thaler JP. High-fat diet feeding causes rapid, non-apoptotic cleavage of caspase-3 in astrocytes. Brain Research. 2013; 1512:97–105. [PubMed: 23548599]
4. Garcia-Caceres C, Yi CX, Tschop MH. Hypothalamic astrocytes in obesity. Endocrinology and Metabolism Clinics of North America. 2013; 42(1):57–66. [PubMed: 23391239]
5. Morari J, Anhe GF, Nascimento LF, de Moura RF, Razolli D, Solon C, et al. Fractalkine (CX3CL1) is involved in the early activation of hypothalamic inflammation in experimental obesity. Diabetes. 2014; 63(11):3770–84. [PubMed: 24947351]
6. Velloso LA, Schwartz MW. Altered hypothalamic function in diet-induced obesity. Int J Obes (Lond). 2011; 35(12):1455–65. [PubMed: 21386802]
7. Valdearcos M, Xu AW, Koliwad SK. Hypothalamic inflammation in the control of metabolic function. Annu Rev Physiol. 2015; 77:131–60. [PubMed: 25668019]

8. Myers MG Jr. Leibel RL, Seeley RJ, Schwartz MW. Obesity and leptin resistance: distinguishing cause from effect. Trends Endocrinol Metab. 2010; 21(11):643–51. [PubMed: 20846876]
9. Parton LE, Ye CP, Coppari R, Enriori PJ, Choi B, Zhang CY, et al. Glucose sensing by POMC neurons regulates glucose homeostasis and is impaired in obesity. Nature. 2007; 449(7159):228–32. [PubMed: 17728716]
10. Kumar RB, Arrone LJ. Hypothalamic Inflammation: Is There Evidence for Human Obesity? Curr Obes Rep.
11. Briellmann RS, Kalnins RM, Berkovic SF, Jackson GD. Hippocampal pathology in refractory temporal lobe epilepsy: T2-weighted signal change reflects dentate gliosis. Neurology. 2002; 58(2):265–71. [PubMed: 11805255]
12. Braffman BH, Zimmerman RA, Trojanowski JQ, Gonatas NK, Hickey WF, Schlaepfer WW. Brain MR: pathologic correlation with gross and histopathology. 2. Hyperintense white-matter foci in the elderly. American journal of roentgenology. 1988; 151(3):559–66. [PubMed: 3261518]
13. Marshall VG, Bradley WG Jr. Marshall CE, Bhoopat T, Rhodes RH. Deep white matter infarction: correlation of MR imaging and histopathologic findings. Radiology. 1988; 167(2):517–22. [PubMed: 3357964]
14. Polman CH, Reingold SC, Edan G, Filippi M, Hartung HP, Kappos L, et al. Diagnostic criteria for multiple sclerosis: 2005 revisions to the "McDonald Criteria". Ann Neurol. 2005; 58(6):840–6. [PubMed: 16283615]
15. Third Report of the National Cholesterol Education Program (NCEP) Expert Panel on Detection, Evaluation, and Treatment of High Blood Cholesterol in Adults (Adult Treatment Panel III) final report. Circulation. 2002; 106(25):3143–3421. [PubMed: 12485966]
16. Herman, CP.; Polivy, J. Restrained eating. In: Stunkard, AJ., editor. Obesity. W.B. Saunders; Philadelphia: 1980. p. 208-225.
17. Stunkard AJ, Messick S. The three-factor eating questionnaire to measure dietary restraint, disinhibition and hunger. J Psychosom Res. 1985; 29(1):71–83. [PubMed: 3981480]
18. Matthews DR, Hosker JP, Rudenski AS, Naylor BA, Treacher DF, Turner RC. Homeostasis model assessment: insulin resistance and beta-cell function from fasting plasma glucose and insulin concentrations in man. Diabetologia. 1985; 28(7):412–9. [PubMed: 3899825]
19. Abel TW, Rance NE. Stereologic study of the hypothalamic infundibular nucleus in young and older women. The Journal of comparative neurology. 2000; 424(4):679–88. [PubMed: 10931489]
20. Hasan KM, Walimuni IS, Abid H, Frye RE, Ewing-Cobbs L, Wolinsky JS, et al. Multimodal quantitative magnetic resonance imaging of thalamic development and aging across the human lifespan: implications to neurodegeneration in multiple sclerosis. The Journal of neuroscience : the official journal of the Society for Neuroscience. 2011; 31(46):16826–32. [PubMed: 22090508]
21. Chung YL, Williams A, Ritchie D, Williams SC, Changani KK, Hope J, et al. Conflicting MRI signals from gliosis and neuronal vacuolation in prion diseases. Neuroreport. 1999; 10(17):3471–7. [PubMed: 10619628]
22. Jackson GD, Williams SR, Weller RO, van Bruggen N, Preece NE, Williams SC, et al. Vigabatrin-induced lesions in the rat brain demonstrated by quantitative magnetic resonance imaging. Epilepsy research. 1994; 18(1):57–66. [PubMed: 8088257]
23. Thaler JP, Guyenet SJ, Dorfman MD, Wisse BE, Schwartz MW. Hypothalamic inflammation: marker or mechanism of obesity pathogenesis? Diabetes. 2013; 62(8):2629–34. [PubMed: 23881189]
24. Yi CX, Al-Massadi O, Donelan E, Lehti M, Weber J, Ress C, et al. Exercise protects against high-fat diet-induced hypothalamic inflammation. Physiology & Behavior. 2012; 106(4):485–90. [PubMed: 22483785]
25. Berkseth KE, Guyenet SJ, Melhorn SJ, Lee D, Thaler JP, Schur EA, et al. Hypothalamic gliosis associated with high-fat diet feeding is reversible in mice: a combined immunohistochemical and magnetic resonance imaging study. Endocrinology. 2014; 155(8):2858–67. [PubMed: 24914942]
26. Jeon BT, Kim KE, Heo RW, Shin HJ, Yi CO, Hah YS, et al. Myeloid-specific deletion of SIRT1 increases hepatic steatosis and hypothalamic inflammation in mice fed a high-fat diet. Metab Brain Dis. 2014; 29(3):635–43. [PubMed: 24756314]

27. Arble DM, Sandoval DA. CNS control of glucose metabolism: response to environmental challenges. Front Neurosci. 2013; 7:20. [PubMed: 23550218]
28. Schwartz MW, Seeley RJ, Tschop MH, Woods SC, Morton GJ, Myers MG, et al. Cooperation between brain and islet in glucose homeostasis and diabetes. Nature. 2013; 503(7474):59–66. [PubMed: 24201279]
29. German JP, Wisse BE, Thaler JP, Oh IS, Sarruf DA, Ogimoto K, et al. Leptin deficiency causes insulin resistance induced by uncontrolled diabetes. Diabetes. 2010; 59(7):1626–34. [PubMed: 20424233]
30. Obici S, Zhang BB, Karkanias G, Rossetti L. Hypothalamic insulin signaling is required for inhibition of glucose production. Nature medicine. 2002; 8(12):1376–82.
31. Lam TK, Gutierrez-Juarez R, Pocai A, Rossetti L. Regulation of blood glucose by hypothalamic pyruvate metabolism. Science. 2005; 309(5736):943–7. [PubMed: 16081739]
32. Hill JW, Elias CF, Fukuda M, Williams KW, Berglund ED, Holland WL, et al. Direct insulin and leptin action on pro-opiomelanocortin neurons is required for normal glucose homeostasis and fertility. Cell metabolism. 2010; 11(4):286–97. [PubMed: 20374961]
33. Posey KA, Clegg DJ, Printz RL, Byun J, Morton GJ, Vivekanandan-Giri A, et al. Hypothalamic proinflammatory lipid accumulation, inflammation, and insulin resistance in rats fed a high-fat diet. American journal of physiology. Endocrinology and metabolism. 2009; 296(5):E1003–12. [PubMed: 19116375]
34. Milanski M, Degasperi G, Coope A, Morari J, Denis R, Cintra DE, et al. Saturated fatty acids produce an inflammatory response predominantly through the activation of TLR4 signaling in hypothalamus: implications for the pathogenesis of obesity. The Journal of neuroscience : the official journal of the Society for Neuroscience. 2009; 29(2):359–70. [PubMed: 19144836]
35. Wisse BE, Schwartz MW. Does hypothalamic inflammation cause obesity? Cell metabolism. 2009; 10(4):241–2. [PubMed: 19808014]
36. Carvalheira JB, Odegaard JI, Chawla A. A new role for the brain in metabolic control. Nat Med. 2014; 20(5):472–3. [PubMed: 24804753]
37. Lemaire JJ, Frew AJ, McArthur D, Gorgulho AA, Alger JR, Salomon N, et al. White matter connectivity of human hypothalamus. Brain Res. 2011; 1371:43–64. [PubMed: 21122799]
38. Wittling W, Block A, Genzel S, Schweiger E. Hemisphere asymmetry in parasympathetic control of the heart. Neuropsychologia. 1998; 36(5):461–8. [PubMed: 9699952]
39. Safer DJ. Diet, behavior modification, and exercise: a review of obesity treatments from a long-term perspective. South Med J. 1991; 84(12):1470–4. [PubMed: 1749981]
40. Sjostrom L, Narbro K, Sjostrom CD, Karason K, Larsson B, Wedel H, et al. Effects of bariatric surgery on mortality in Swedish obese subjects. N Engl J Med. 2007; 357(8):741–52. [PubMed: 17715408]

STUDY IMPORTANCE QUESTIONS

What is already known about this subject?

- Rodent models suggest diet-induced obesity is associated with inflammation and gliosis within the hypothalamus.
- The hypothalamus is critical in the control of energy balance and glucose metabolism.

What does your study add?

- The first prospective report on detection of gliosis in the human hypothalamus both *in vivo* and in postmortem samples.
- Radiologic evidence that gliosis in humans is associated with insulin resistance, independent of the level of adiposity.

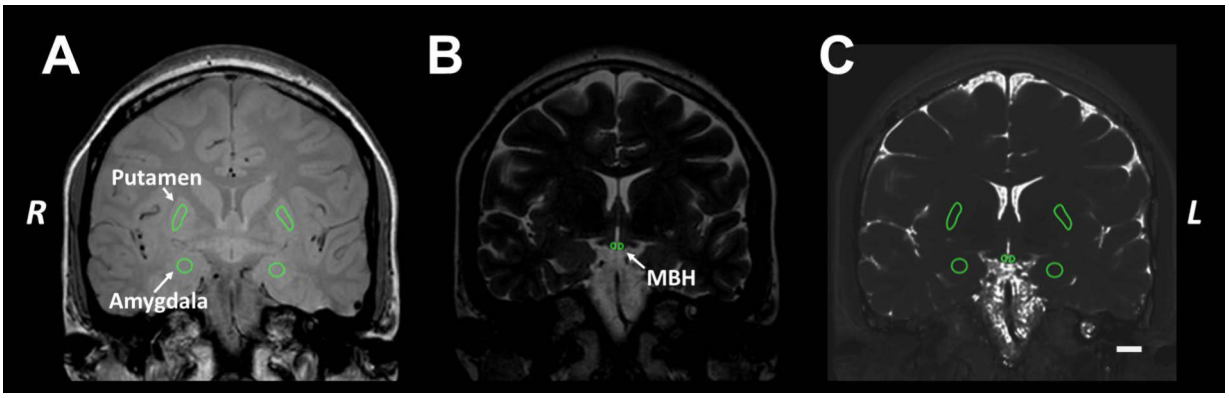

Figure 1. Measurement of T2 relaxation time

Regions of interest (ROIs) were placed on high resolution coronal sections (A: TE 20 & B: TE 170 ms) then transferred to a parametric map of T2 relaxation times (C) derived from the multi-echo sequence to measure the mean (SD) T2 relaxation time within each ROI. The MBH ROI was placed adjacent to the 3rd ventricle to encompass the location of the arcuate nucleus. Reference ROIs were placed in the amygdala and putamen. The ROI areas were: MBH ~3.9 mm^2 (with corresponding tissue volume 9.75 mm^3), putamen ~3.56 mm^2 (8.90 mm^3), and amygdala ~2.97 mm^2 (7.43mm^3). Scale bar in C represents 1 cm. MBH: mediobasal hypothalamus.

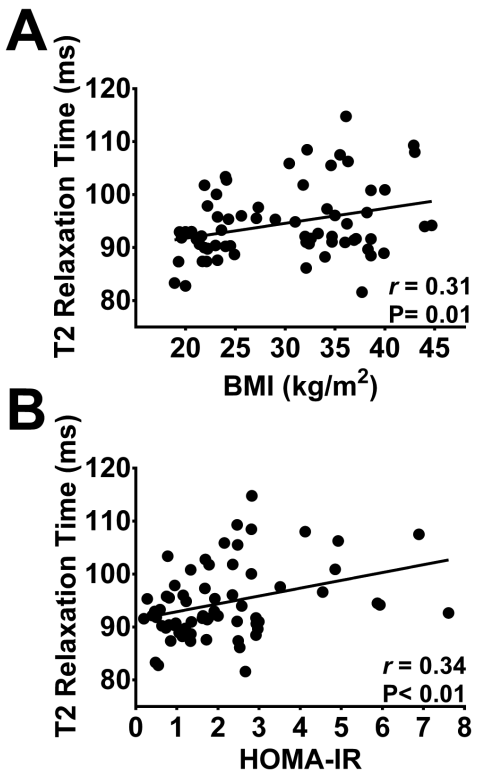

Figure 2. Hypothalamic T2 relaxation time, adiposity and insulin resistance

Longer T2 relaxation times in the left mediobasal hypothalamus are associated with higher BMI (A) and higher HOMA-IR scores (B). N=67.

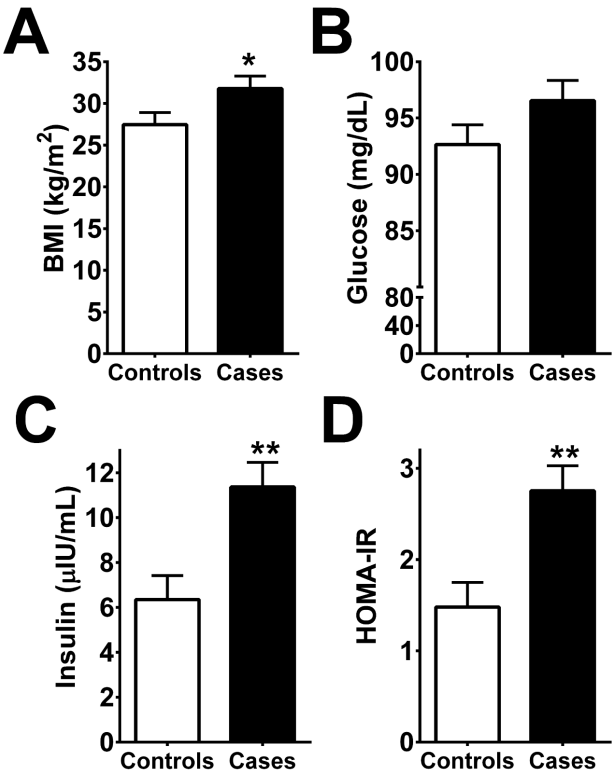

Figure 3. Nested case-control study of radiologic evidence of gliosis

Cases were identified as the tertile with the highest mean T2 relaxation time in the left mediobasal hypothalamus (MBH). Cases with radiologic evidence of gliosis have higher BMIs (A), fasting insulin concentrations (C) and HOMA-IR (D) but not fasting glucose concentrations (B). Data are least square means ± SEM; P-values determined from linear regression. Data are adjusted for sex and age. N=23 (Controls), 22 (Cases). *****P<0.05, ******P<0.01.

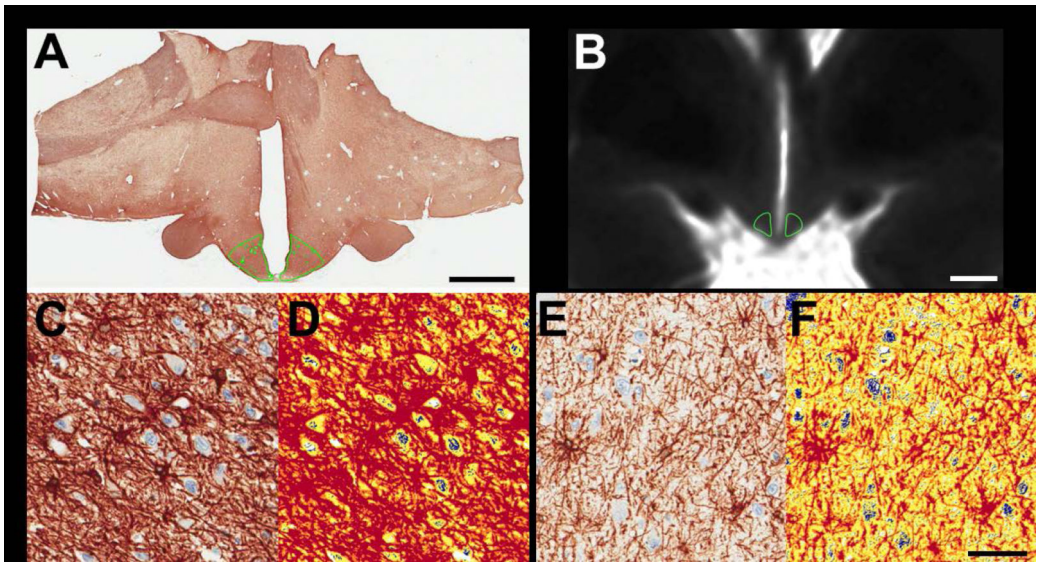

Figure 4. Representative images of mediobasal hypothalamus (MBH) ROI and GFAP staining in autopsy samples

Coronal brain slices that included the hypothalamus were imaged, sectioned, stained for glial fibrillary acidic protein (GFAP) via immunohistochemistry and digitally scanned. ROIs were placed on digital images (A, captured at 0.4X, scale bar represents 5 mm) and on a parametric map of T2 relaxation times derived from the multi-echo sequence for radiologic analysis (B, scale bar represents 5 mm). In both cases, the MBH ROI was placed adjacent to the 3rd ventricle to encompass the location of the arcuate nucleus. Panels C-D show representative sections through the MBH from a brain slice with a high MBH T2 relaxation time and panels E-F are derived from a brain slice with a low MBH T2 relaxation time. Images in panels C and E depict immunostaining for GFAP (brown) and hematoxylin (blue) whereas panels D and F depict the identical region processed with digital color deconvolution software to measure staining intensity. Pseudocolors in D and F represent staining intensity (blue or white=no stain, yellow=low intensity and red=moderate or high intensity). Images in C-F captured at 40X; scale bar = 50 μm.

TABLE 1

	Controls	Cases
N	23	22
Women, *%*	61	41
Age, *years*	31 (10)	33 (11)
Weight, *kg*	82 (25)	97 (23) *
Lifetime max weight, *kg*	87 (28)	101 (24) #
Weight reduced from max, *%*	5.9 (5.0)	4.3 (4.5)
Obese, *%*	39	64
TFEQ cognitive restraint score	12 (4.3)	14 (3.4)
TFEQ emotional eating score	7.0 (2.4)	6.4 (2.4)
TFEQ uncontrolled eating score	19 (5.3)	20 (5.1)
Restraint Scale score	15 (5.3)	16 (5.1)
Physical activity, median *MET-min/wk*†	3492 (1515-5598)	2634 (1026-4293)
Time spent sitting, median *min/day*†	420 (360-690)	480 (300-600)

†Data are mean (SD) or †median (Interquartile Range). TFEQ: Three Factor Eating Questionnaire.

*P<0.05 vs. Controls,

#P=0.08 vs. Controls.